Guidance of Quadrotor Unmanned Aerial Vehicles via Adaptive Multiple-Surface Sliding Mode Control

Gian Paolo Incremona and Antonella Ferrara

Abstract— **In many application domains, navigation of unmanned aerial vehicles (UAVs) requires a planar flight to move along a desired path or to track a moving object under uncertain conditions. In this paper, we propose a robust control approach for quadrotor UAVs performing a nonholonomic-like navigation with a predefined velocity based guidance law. Specifically, the quadrotor model is first recast in the framework of nonholonomic systems, and then an adaptive multiple-surface sliding mode approach, with suboptimal second order sliding mode control, is applied. The robustness features of the proposed approach are discussed and assessed in simulation.**

Index Terms— **Sliding mode control, unmanned aerial vehicles, nonholonomic systems.**

I. Introduction

UAV applications are nowadays more and more present in many spheres of human activities, such as civil usage (e.g., shipping and delivery, geographic mapping, human health), agriculture tasks (e.g., plant prevention spray, irrigation system), or military scope (e.g., surveillance and security), see [1]. Moreover, UAVs can be categorized depending on their structure and size. Typically, two main classes can be considered: the fixed-wing vehicles [2], capable of flying by using wings, and multi-rotors such as quadrotors [3]. In this paper, we focus on guidance control of quadrotor UAVs. The latter are vehicles with a symmetric body frame and four propellers, whose model is captured by a 6-degrees-of-freedom mechanical system, with three translational and three rotational variables, and governed by four inputs corresponding to the propeller rotational speeds. Then, it is clear that it is an underactuated system. A possible way to control such a system is to consider only three translational and one rotational degrees of freedom. However, the resulting system contains coupled and highly nonlinear dynamics which can be further affected by parametric uncertainties, or external disturbances [4], thus requiring appropriate robust controllers.

The literature on quadrotor UAVs control is indeed wide, covering many domains, as stabilization, navigation or obstacle avoidance, and many different methodologies are exploited. The so-called flatness theory is for instance used in [5] to linearize the quadrotor model by using a feed-forward and a feedback scheme. A flatness-based passivity control is proposed instead in [6], while a flatness based scheme with model predictive controllers is presented in [7], [8]. Among many others, nonlinear control methodologies based on adaptive controllers and online model identification are those discussed in [9] or [10], respectively.

Despite a wide literature, several issues still need to be investigated, such as requirement of robustness in front of parameter uncertainties and external disturbances. For these reasons, sliding mode control looks promising [11]. However, the adoption of sliding mode approaches in rigorous and comprehensive fashion requires a preliminary reformulation of the quadrotor control model depending also on the application. As an example, the application of the flatness theory provides a transformation to achieve a linear system in normal form, eligible to design a sliding mode controller for trajectory tracking problems, see e.g., [5]. In [12] the dynamical model of the quadrotor is split into a fully actuated subsystem and an underactuated subsystem, and a second order sliding mode with switching surface is designed. A hierarchical control structure with an inner-outer loop framework is proposed in [13] to design a continuous nonsingular terminal sliding mode control, while an adaptive super twisting in presence of input-delay, model uncertainty and wind disturbance is adopted in [14].

In this paper, in analogy with [15], we consider the specific scenario where a nonholonomic-like navigation is required and the quadrotor flies on a plane as a fixed-wing UAV, as requested for instance for inspection, indoor navigation or filming. Therefore, this formation differs from those in [5], [12]–[14], and inspired by [16], an adaptive multiple-surface sliding mode control with a suboptimal second order sliding mode control algorithm [17] is proposed. Instead, differently from [15], where velocity and acceleration based guidance strategies are introduced and no disturbances are taken into account, the objective of this work is to provide a novel robust approach for the nonoholomic UAV system in order to follow, in uncertain conditions, a desired velocity based guidance law, whose design phase is beyond the scope of the paper. Since the vehicle is assumed to get any configuration in employing only the heading, the forward or the vertical motions, the rolling angle is forced to zero and yaw and pitch control are taken into account relying on a nonholonmic formulation of the quadrotor model.

The paper is organized as follows. In Section II the quadrotor model and the navigation problem are discussed. In Section III the model is recast into the nonholonomic framework, while in Section IV the proposed sliding mode

This is the final version of the accepted paper submitted for inclusion in the Proceedings of the American Control Conference 2023, San Diego, CA, USA, May–June 2023, doi:10.23919/ACC55779.2023.10156354. Gian Paolo Incremona is with Dipartimento di Elettronica, Informazione e Bioingegneria, Politecnico di Milano, 20133 Milan, Italy (e-mail: *gianpaolo.incremona@polimi.it*).

Antonella Ferrara is with the Dipartimento di Ingegneria Industriale e dell'Informazione, University of Pavia, 27100, Pavia, Italy (e-mail: *antonella.ferrara@unipv.it*).

approach is presented. Finally, in Section V some simulations are shown, and some conclusions are drawn in Section VI.

Notation: The main notation and operators used in the paper are recalled hereafter. Given a vector $\boldsymbol{x} \in \mathbb{R}^n$, its transpose is $\boldsymbol{x}'$, while the corresponding unit vector is indicated as $\mathbf{x}$. Given a matrix $\boldsymbol{P} \in \mathbb{R}^{n\times n}$, $\boldsymbol{P} > 0$ indicates that it is positive definite. Let $s \in \mathbb{R}$ be a signal, the function $\mathrm{sign}(s)$ is defined as -1 if $s < 0$, 1 if $s > 0$, and $[-1, 1]$ if $s = 0$. Moreover, given the signal $\alpha \in \mathbb{R}$, let $c_\alpha := \cos(\alpha)$ and $s_\alpha := \sin(\alpha)$.

II. Problem Setting

In this section, the conventional quadrotor UAV model is first introduced, and the considered navigation control problem is formulated.

A. Modelling

In order to introduce the conventional description of the dynamical model of the quadrotor UAV, a fixed world reference $\mathcal{W}$, given by the triad $\mathbf{x}_\mathrm{W}$, $\mathbf{y}_\mathrm{W}$, $\mathbf{z}_\mathrm{W}$, and a body reference frame $\mathcal{B}$, given by the triad $\mathbf{x}_\mathrm{B}$, $\mathbf{y}_\mathrm{B}$, $\mathbf{z}_\mathrm{B}$, are used (see Figure 1). Frame $\mathcal{B}$ is attached to the UAV center of mass with $\mathbf{z}_\mathrm{B}$ perpendicular to the plane of the rotors pointing vertically up. Moreover, in the model definition, we assume that low velocities make the air drag, ground effects and aeroelasticity negligible, as well as actuator dynamics is neglected. Additionally, small angles of movement are assumed.

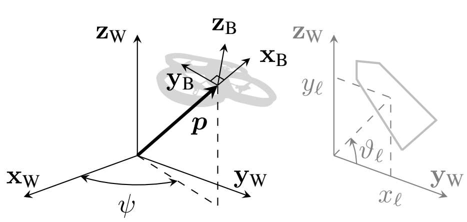

Fig. 1. Quadrotor frames and nonholonomic navigation projection.

Now, consider the conventional ZXY Euler convention with angles $\boldsymbol{\varphi} := [\phi, \theta, \psi]'$ to capture the rotation with respect to the world frame $\mathcal{W}$, while the position of frame $\mathcal{B}$ with respect to $\mathcal{W}$ is given by $\boldsymbol{p} := [x, y, z]'$. Let $\boldsymbol{\omega} = [\omega_1, \omega_2, \omega_3, \omega_4]'$ contain the velocities of rotors having inertia J, and $\boldsymbol{w} := [p, q, r]'$ be the rotational velocity such that the simplification $\boldsymbol{w} = [\dot{\phi}, \dot{\theta}, \dot{\psi}]'$ holds due to small angles of movements. Moreover, let ${}^{\mathcal{W}}\mathbf{R}_\mathcal{B}$ be the rotational matrix between the frames $\mathcal{B}$ and $\mathcal{W}$, and $\mathbf{S}(\boldsymbol{w})$ be the skew-symmetric matrix given by

$$\mathbf{S}(\boldsymbol{w}) := \begin{bmatrix} 0 & -\dot{\psi} & \dot{\theta} \\ \dot{\psi} & 0 & -\dot{\phi} \\ -\dot{\theta} & \dot{\phi} & 0 \end{bmatrix}.$$

Therefore, exploiting the Newton's and Euler's equations of motion, the quadrotor UAV obeys to

$$\begin{aligned} m\ddot{\boldsymbol{p}} &= -mg\mathbf{z}_\mathrm{W} + {}^{\mathcal{W}}\mathbf{R}_\mathcal{B}(\tau_1 + \tau_{d1})\mathbf{z}_\mathrm{B} \\ \mathbf{I}\,\dot{\boldsymbol{w}} &= \boldsymbol{\tau}_2 + \boldsymbol{\tau}_{d2} - \mathbf{S}(\boldsymbol{w})\left(\mathbf{I}\,\boldsymbol{w} - J\omega_\mathrm{r}\mathbf{z}_\mathrm{B}\right), \end{aligned} \tag{1}$$

where m and $\mathbf{I} = \mathrm{diag}(I_x, I_y, I_z)$ are quadrotor mass and inertia tensor expressed in body frame, respectively, $\omega_\mathrm{r} = -\omega_1 + \omega_2 - \omega_3 + \omega_4$, g is the gravitational constant, while τ_1 and $\boldsymbol{\tau}_2$ are the inputs

$$\tau_1 := \sum_{i=1}^{4} F_i, \quad \boldsymbol{\tau}_2 := \begin{bmatrix} L(F_2 - F_4) \\ L(F_3 - F_1) \\ M_1 + M_3 - M_2 - M_4 \end{bmatrix} = \begin{bmatrix} \tau_2 \\ \tau_3 \\ \tau_4 \end{bmatrix},$$

with L being the length of each body arm, F_i and M_i, $i = 1, \dots, 4$, being thrust forces and reaction moments provided by propellers. The matched disturbances are instead indicated as τ_{d1} and $\boldsymbol{\tau}_{d2} = [\tau_{d2}, \tau_{d3}, \tau_{d4}]'$. Explicitly writing the equations in (1), one has

$$\begin{aligned} \ddot{x} &= (\tau_1 + \tau_{d1})\frac{c_\psi s_\theta c_\phi + s_\psi s_\phi}{m} \\ \ddot{y} &= (\tau_1 + \tau_{d1})\frac{s_\psi s_\theta c_\phi + c_\psi s_\phi}{m} \\ \ddot{z} &= -g + (\tau_1 + \tau_{d1})\frac{c_\theta c_\phi}{m} \\ \ddot{\phi} &= \frac{\tau_2 + \tau_{d2}}{I_x} + \dot{\theta}\dot{\psi}\frac{I_y - I_z}{I_x} - \frac{J}{I_x}\dot{\theta}\omega_\mathrm{r} \\ \ddot{\theta} &= \frac{\tau_3 + \tau_{d3}}{I_y} + \dot{\phi}\dot{\psi}\frac{I_z - I_x}{I_y} + \frac{J}{I_y}\dot{\phi}\omega_\mathrm{r} \\ \ddot{\psi} &= \frac{\tau_4 + \tau_{d4}}{I_z} + \dot{\phi}\dot{\theta}\frac{I_x - I_y}{I_z}. \end{aligned} \tag{2}$$

B. Formulation of the navigation problem

In this paper, we are interested in designing a quadrotor guidance control taking care of the heading, forward and vertical motions of the UAV. Differently from classical guidance control with longitudinal and lateral motions, in other applications, such as object tracking or inspection, a nonholonomic-like navigation is preferable.

Therefore, having in mind this scenario, we assume the rolling angle steered to zero by applying a suitable controller (in whatever appropriate sense, e.g., see [18]), i.e., $\phi = \dot{\phi} = 0$. As a consequence, the previous model (2) can be written in a reduced form as

$$\begin{aligned} \ddot{x} &= \tau_1\frac{c_\psi s_\theta}{m} + \underbrace{\tau_{d1}\frac{c_\psi s_\theta}{m}}_{d_x} \\ \ddot{y} &= \tau_1\frac{s_\psi s_\theta}{m} + \underbrace{\tau_{d1}\frac{s_\psi s_\theta}{m}}_{d_y} \\ \ddot{z} &= \tau_1\frac{c_\theta}{m} + \underbrace{\tau_{d1}\frac{c_\theta}{m} - g}_{d_z} \\ \ddot{\theta} &= \frac{\tau_3}{I_y} + \underbrace{\frac{\tau_{d3}}{I_y}}_{d_\theta} \\ \ddot{\psi} &= \frac{\tau_4}{I_z} + \underbrace{\frac{\tau_{d4}}{I_z}}_{d_\psi}. \end{aligned} \tag{3}$$

Following the same reasoning in [15], we consider now the following forward linear speed rate, i.e.,

$$\dot{v} = \tau_1\frac{s_\theta}{m}. \tag{4}$$

Hence, the reduced system (3) becomes

$$\ddot{x} = \dot{v}c_\psi + d_x, \quad \ddot{y} = \dot{v}s_\psi + d_y, \quad \ddot{z} = \tau_1\frac{c_\theta}{m} + d_z, \\ \ddot{\theta} = \frac{\tau_3}{I_y} + d_\theta, \quad \ddot{\psi} = \frac{\tau_4}{I_z} + d_\psi, \tag{5}$$

for which the following assumption needs to be introduced.

$\boldsymbol{\mathcal{A}_1}$: The disturbance terms d_x, d_y, d_z, d_θ and d_ψ are assumed bounded with known bounds.

Note that the boundedness of the considered disturbances is reasonable in practice due to the physical nature of the quadrotor system and of possible torque deviations.

We are now in a position to design the controller to make the speed of the quadrotor track the desired speed $(\dot{x}^\star, \dot{y}^\star)$, generated by an appropriate guidance law, and with desired angles $\psi^\star$ and $\theta^\star$. Note that, in this work, the altitude z will in turn depend on τ_1 and on pitch angle θ.

III. Recasting the Quadrotor Model into the Nonholonomic Framework

Before introducing the proposed control approach, we need to reformulate the quadrotor model into a suitable nonholonomic framework eligible for the design of the sliding mode strategy presented in this paper. By adopting a suitable change of variables, let $x_\ell := \dot{x}$, $y_\ell := \dot{y}$, $z_\ell := \dot{z}$, $\vartheta_\ell := \psi$, and $\theta_\ell := \theta$ be the new set of variables, such that one has

$$\begin{aligned} \dot{x}_\ell &= \dot{v}c_{\vartheta_\ell} + d_x \\ \dot{y}_\ell &= \dot{v}s_{\vartheta_\ell} + d_y \\ \dot{z}_\ell &= \tau_1\frac{c_{\theta_\ell}}{m} + d_z \\ \ddot{\theta}_\ell &= \frac{\tau_3}{I_y} + d_\theta \\ \ddot{\vartheta}_\ell &= \frac{\tau_4}{I_z} + d_\psi, \end{aligned} \tag{6}$$

Now, consider further auxiliary state variables given by

$$\begin{aligned} x_0 &:= \vartheta_\ell - \psi^\star, \\ x_1 &:= (x_\ell - \dot{x}^\star)s_{x_0} - (y_\ell - \dot{y}^\star)c_{x_0}, \\ x_2 &:= (x_\ell - \dot{x}^\star)c_{x_0} + (y_\ell - \dot{y}^\star)s_{x_0}, \\ x_3 &:= z_\ell, \\ x_4 &:= \theta_\ell - \theta^\star, \ x_5 = \dot{x}_4, \end{aligned}$$

and the inputs

$$u_0 := \dot{\vartheta}_\ell - \dot{\psi}^\star, \ u_1 := \dot{v},$$

so that (6) becomes the following nonholonomic system,

$$\begin{cases} \dot{x}_0 = u_0 \\ \dot{x}_1 = x_2u_0 + \delta_1 \\ \dot{x}_2 = d_2u_1 + \delta_2 \end{cases} \tag{7a}$$

$$\dot{x}_3 = \tau_1\frac{c_{\theta_\ell}}{m} + d_z \tag{7b}$$

$$\begin{cases} \dot{x}_4 = x_5 \\ \dot{x}_5 = \frac{\tau_3}{I_y} + d_\theta - \ddot{\theta}^\star \end{cases} \tag{7c}$$

$$\dot{u}_0 = \frac{\tau_4}{I_z} + d_\psi - \ddot{\psi}^\star, \tag{7d}$$

where $d_2 := c_\psi c_{x_0} + s_\psi s_{x_0}$ is known such that $-1 \le d_2 \le 1$, while $\delta_1 := u_1(c_\psi s_{x_0} - s_\psi c_{x_0}) + (d_x - \ddot{x})s_{x_0} - (d_y - \ddot{y})c_{x_0}$, $\delta_2 := (d_x - \ddot{x}^\star)c_{x_0} + (d_y - \ddot{y}^\star)s_{x_0} - x_1u_0$.

Note that the dynamics of x_1 and x_3 implicitly depend on u_1, which will be designed as a bounded signal, while the dynamics in (7c) implies the stabilization of the pitch angle θ by designing a suitable (in whatever appropriate sense) controller for the input τ_3. Therefore, in the following, let us focus on the stabilization of the new states x_0, x_1 and x_2 in (7a). Inspecting the equations, it is clear that, when the control u_0 converges to zero, this makes the system uncontrollable via u_1. To overcome this issue a discontinuous state scaling [19], which has the capability to not make x_0 converge to zero before x_1 and x_2, is applied, that is $z_1 := \frac{x_1}{x_0}$ and $z_2 := x_2$. The resulting system is

$$\dot{x}_0 = u_0 \tag{8a}$$

$$\begin{cases} \dot{z}_1 = u_0\frac{z_2}{x_0} + \Delta_1 \\ \dot{z}_2 = d_2u_1 + \Delta_2, \end{cases} \tag{8b}$$

with $\Delta_i := \frac{\delta_i}{x_0^{n-i}}$ being uncertain terms, such that the following assumption holds.

$\boldsymbol{\mathcal{A}_2}$: All the unknown functions, generally denoted as $h(t)$, fulfill the Dirichlet conditions [20], i.e., they can be written into Fourier series in the time interval $[0, T_\mathrm{s}]$, $T_\mathrm{s} > 0$, as

$$h(t) = \boldsymbol{w}'\boldsymbol{b}(t) + \epsilon, \tag{9}$$

with

$$\begin{aligned} \boldsymbol{w}' &:= [a_0, a_1, \ldots, a_N], \\ \boldsymbol{b}'(t) &:= \left[1, c_{\frac{2\pi t}{T_\mathrm{s}}}, s_{\frac{2\pi t}{T_\mathrm{s}}}, \ldots, c_{\frac{2N\pi t}{T_\mathrm{s}}}, s_{\frac{2N\pi t}{T_\mathrm{s}}}\right], \\ \epsilon &:= \sum_{j=N+1}^{\infty}\left(a_jc_{\frac{2j\pi t}{T_\mathrm{s}}} + \beta_js_{\frac{2j\pi t}{T_\mathrm{s}}}\right). \end{aligned}$$

Therefore, making reference to $\boldsymbol{\mathcal{A}_2}$, for larger value of N basis functions, any unknown function $h(t)$ can be approximated as

$$\hat{h}(t) = \hat{\boldsymbol{w}}'\boldsymbol{b}(t), \tag{10}$$

where $\hat{\boldsymbol{w}}$ is an estimate of $\boldsymbol{w}$, and $h - \hat{h} = \boldsymbol{w}'\boldsymbol{b} - \hat{\boldsymbol{w}}'\boldsymbol{b} + \epsilon$, with ϵ being the approximation error.

IV. Proposed Multiple-Surface Sliding Mode Control

In this section the proposed control approach is introduced. First, the x_0-subsystem (8a) is considered, and then a sliding mode controller of suboptimal type is designed for the z-subsystem (8b).

A. Control of the x_0-subsystem

Before introducing the control law for the x_0-subsystem (8a), the following assumption has to be introduced.

$\boldsymbol{\mathcal{A}_3}$: The initial condition for subsystem (8a) is $x_0(t_0) \neq 0$, with t_0 being the initial time instant.

Note that $\mathcal{A}_3$ is instrumental to apply the discontinuous state scaling in (8) and the case $x_0(t_0) = 0$ requires a preliminary controller to move x_0 away from the origin.

By choosing a Lyapunov function as

$$V_0 = \frac{1}{2}x_0^2, \tag{11}$$

substituting (8a), it is possible to verify that $\dot{V}_0 = u_0 x_0$. Hence, by choosing the control u_0 as

$$u_0 = -k_0 x_0, \tag{12}$$

with $k_0 > 0$, one has $\dot{V}_0 = -k_0 x_0^2 < 0$, that is x_0 is asymptotically regulated to zero.

B. Multiple-surface design for the z-subsystem

Consider now the z-subsystem (8b) for which we define the following sliding surfaces

$$s_1 := z_1 \tag{13a}$$
$$s_2 := z_2 - \alpha_1, \tag{13b}$$

where α_1 is a virtual control designed as

$$\alpha_1 := \frac{k_1 s_1 + \hat{\Delta}_1}{k_0}, \tag{14}$$

where $k_1 > 0$, and $\hat{\Delta}_1$ is the estimate of Δ_1 as in (10). The following result can be proved.

Proposition 1: Given the sliding variable s_1 in (13a), and the dynamics of z_1 as in (8b), if $\mathcal{A}_2$ holds, and both ϵ_1 and s_2 tend to zero, then $\lim_{t\to\infty} s_1 = 0$.

Proof: Consider now a Lyapunov function

$$V_1 = \frac{1}{2}s_1^2 + \frac{1}{2}\tilde{\boldsymbol{w}}_1'\boldsymbol{Q}_1\tilde{\boldsymbol{w}}_1, \tag{15}$$

with $\tilde{\boldsymbol{w}}_1 = \boldsymbol{w}_1 - \hat{\boldsymbol{w}}_1$ and $\boldsymbol{Q}_1 = \boldsymbol{Q}_1' > 0$. Posing $\hat{\boldsymbol{w}}_1 := \boldsymbol{Q}_1^{-1}\boldsymbol{b}s_1$, and exploiting (9), (10), one has

$$\begin{aligned}
\dot{V}_1 &= -s_1 k_0 z_2 + s_1\Delta_1 + \tilde{\boldsymbol{w}}_1'\boldsymbol{b}s_1 \\
&= -s_1 k_0(s_2 + \alpha_1) + s_1\Delta_1 - (\boldsymbol{w}_1 - \hat{\boldsymbol{w}}_1)\boldsymbol{b}s_1 \\
&= -k_1 s_1^2 - k_0 s_1 s_2 - s_1(\hat{\Delta}_1 - \Delta_1) - (\boldsymbol{w}_1 - \hat{\boldsymbol{w}}_1)\boldsymbol{b}s_1 \\
&= -k_1 s_1^2 - k_0 s_1 s_2 + \epsilon_1 s_1.
\end{aligned}$$

Under the assumption $\mathcal{A}_2$, with ϵ_1 and s_2 tending to zero, the time-derivative is $\dot{V}_1 = -k_1 s_1^2 < 0$. Hence, one has that s_1 tends asymptotically to zero, which concludes the proof. ■

At this point, we need to prove that the sliding variable s_2 is steered to zero. Hence, consider now s_2 and compute its time-derivative, i.e.,

$$\begin{aligned}
\dot{s}_2 = \dot{z}_2 &= d_2 u_1 + \Delta_2 - \dot{\alpha}_1 \\
&= d_2 u_1 + \Delta_2 - \frac{\dot{\hat{\Delta}}_1}{k_0} - \frac{k_1}{k_0}\Delta_1 + k_1 z_2 \\
&= d_2 u_1 + \bar{\Delta}_2 + k_1 z_2,
\end{aligned} \tag{16}$$

where $\bar{\Delta}_2 := \Delta_2 - \frac{\dot{\hat{\Delta}}_1}{k_0} - \frac{k_1}{k_0}\Delta_1$ is the lumped uncertain term. The control input u_1 is designed as

$$u_1 = \bar{u}_1 + \tilde{u}_1, \tag{17}$$

where $\bar{u}_1$ is a stabilizing law given by

$$\bar{u}_1 := -\frac{1}{d_2}(k_2 s_2 + \hat{\bar{\Delta}}_2 + k_1 z_2), \tag{18}$$

with $k_2 > 0$. The second component $\tilde{u}_1$ is instead aimed at robustifying the whole control as discussed in the following.

Proposition 2: Given the sliding variables s_2 in (13b), and the dynamics of z_1 and z_2 as in (8b), if $\mathcal{A}_2$ holds, and both ϵ_2 and $\tilde{u}_1$ are bounded, then s_2 is also bounded.

Proof: Consider now a Lyapunov function

$$V_2 = \frac{1}{2}s_2^2 + \frac{1}{2}\tilde{\boldsymbol{w}}_2'\boldsymbol{Q}_2\tilde{\boldsymbol{w}}_2, \tag{19}$$

with $\tilde{\boldsymbol{w}}_2 = \boldsymbol{w}_2 - \hat{\boldsymbol{w}}_2$ and $\boldsymbol{Q}_2 = \boldsymbol{Q}_2' > 0$. Posing $\hat{\bar{\Delta}}_2 = \hat{\boldsymbol{w}}_2'\boldsymbol{b}$ and $\bar{\Delta}_2 = \boldsymbol{w}_2'\boldsymbol{b} + \epsilon_2$, and letting $\dot{\hat{\boldsymbol{w}}}_2 := \boldsymbol{Q}_2^{-1}\boldsymbol{b}s_2$, compute the time-derivative of V_2, i.e.,

$$\begin{aligned}
\dot{V}_2 &= s_2\left(d_2 u_1 + \bar{\Delta}_2 + k_1 z_2\right) - \tilde{\boldsymbol{w}}_2'\boldsymbol{b}s_2 \\
&= s_2\left(d_2\bar{u}_1 + d_2\tilde{u}_1 + \bar{\Delta}_2 - (\boldsymbol{w}_2 - \hat{\boldsymbol{w}}_2)\boldsymbol{b} + k_1 z_2\right) \\
&= s_2\left(d_2\tilde{u}_1 - \hat{\bar{\Delta}}_2 + \bar{\Delta}_2 - (\boldsymbol{w}_2 - \hat{\boldsymbol{w}}_2)\boldsymbol{b} - k_2 s_2\right) \\
&= -k_2 s_2^2 + s_2 d_2\tilde{u}_1 + \epsilon_2 s_2.
\end{aligned}$$

Hence, under the assumption that $\tilde{u}_1$ and ϵ_2 are bounded, relying on the concept of input-to-state stability, also s_2 is bounded. ■

C. Suboptimal sliding mode control signal $\tilde{u}_1$

Given the results in the previous subsection, it is now instrumental to design a suitable bounded control law $\tilde{u}_1$ to steer s_2 to zero despite the presence of uncertain terms. In this case, the natural choice to design a sliding mode control law is to select the sliding variable as s_2 in (13b). Although the relative degree is 1 and a first order sliding mode control naturally applies, as evident from (16), a second order sliding mode is hereafter designed. Let us compute the second-order time derivative of the sliding variable, i.e.,

$$\ddot{s}_2 = d_2\dot{\bar{u}}_1 + d_2\dot{\tilde{u}}_1 + \dot{d}_2 u_1 + \dot{\bar{\Delta}}_2 + k_1(d_2 u_1 + \Delta_2). \tag{20}$$

Posing $\sigma_1 = s_2$ and $\sigma_2 = \dot{s}_2$, a second-order auxiliary system can be introduced, that is

$$\begin{aligned}
\dot{\sigma}_1 &= \sigma_2 \\
\dot{\sigma}_2 &= f + d_2\nu \\
\dot{\tilde{u}}_1 &= \nu,
\end{aligned} \tag{21}$$

where the drift term is given by $f := d_2\dot{\bar{u}}_1 + \dot{d}_2 u_1 + \dot{\bar{\Delta}}_2 + k_1(d_2 u_1 + \Delta_2)$, and, by virtue of assumption $\mathcal{A}_1$, the following assumption, required to design the proposed sliding mode controller, holds.

$\mathcal{A}_4$: There exists a known constant $\bar{f}$ such that the following inequality holds

$$|f| \leq \bar{f}. \tag{22}$$

Making reference to [17], the auxiliary control law is chosen as

$$\nu(t) := -\gamma\,\mathrm{sign}(d_2)\,\mathrm{sign}\left(\sigma_1(t) - \frac{1}{2}\sigma_{1\,\max}\right), \tag{23}$$

with $\gamma > 0$, and $\sigma_{1\,\max}$ being the most recent extremal value such that $\dot{\sigma}_1(t) = 0$, which can be retrieved by an estimation mechanism (see, e.g., [21]). The following result can be proved.

Proposition 3: Given the auxiliary system (21), controlled via (23), if $\boldsymbol{\mathcal{A}_4}$ holds and

$$\gamma > \max\left\{\bar{f}, 2\bar{f}\right\},$$

then the auxiliary system trajectory converges to zero in a finite time $\bar{t} \geq t_0$, hence $\sigma_1(t) = s_2(t) = 0, \forall\, t \geq \bar{t}$.

Proof: The proof directly follows from [17]. ∎

D. Main results

In this section, the main result considering the navigation problem in §II-B is stated.

Theorem 4: Consider the subsystem (7a) controlled via control laws (12) and (17) with (18), (23) and virtual input (14). If $\boldsymbol{\mathcal{A}_1}$, $\boldsymbol{\mathcal{A}_2}$, $\boldsymbol{\mathcal{A}_3}$ and $\boldsymbol{\mathcal{A}_4}$ hold and $\epsilon_i \approx 0$, $i = 1, 2$, then the trajectories of subsystem (7a) are ultimately bounded.

Proof: The proof directly follows by selecting a Lyapunov function equal to

$$V = V_0 + V_1 = \frac{1}{2}x_0^2 + \frac{1}{2}s_1^2 + \frac{1}{2}\tilde{\boldsymbol{w}}_1'\boldsymbol{Q}_1\tilde{\boldsymbol{w}}_1. \qquad (24)$$

Under assumptions $\boldsymbol{\mathcal{A}_1}$, $\boldsymbol{\mathcal{A}_2}$, $\boldsymbol{\mathcal{A}_3}$ and $\boldsymbol{\mathcal{A}_4}$, and $\epsilon_i \approx 0$, $i = 1, 2$, the time derivative of V is

$$\dot{V} = -k_0 x_0^2 - k_1 s_1^2 < 0, \qquad (25)$$

from which x_0 and $s_1 = z_1$, hence also x_1, asymptotically tend to zero. Then, by virtue of Proposition 3 and control law (23), s_2 is steered to zero in finite time. This implies $z_2 = x_2 = \alpha_1$ such that $\lim_{t\to\infty} x_2(t) = \frac{\hat{\Delta}_1}{k_0}$, which is bounded, thus concluding the proof. ∎

Note that, as mentioned in §III, the state x_4 is steered to zero, which implies $\theta = \theta^\star$, while by virtue of Theorem 4, if $x_0 = x_1 = 0$, it is clear that one in turn has $\dot{y} = \dot{y}^\star$ and $\psi = \psi^\star$, while from x_2 one has $\dot{x} = \dot{x}^\star + \varepsilon(u_1, \psi^\star, \theta, \ddot{y})$, with $\varepsilon(u_1, \psi^\star, \theta, \ddot{y})$ being a bounded function such that $\varepsilon(u_1, 0, 0, 0) = 0$.

V. Simulation Tests

In this section, the proposed adaptive multiple-surface sliding mode control strategy is validated in simulation.

A. Scenario

In order to assess the proposal, the model of the quadrotor captured by system (3) is implemented in MATLAB-SIMULINK© together with (5) and (7). Moreover, making reference to the model adopted in [5], the physical parameters are those reported in Table I, with all the assumptions discussed in §II-A. In the considered navigation scenario, the quadrotor has to perform a linear motion, starting at $t_0 = 0$ from coordinates $[x(0), y(0), z(0)]' = [2.5, 0, 6]'\,\mathrm{m}$ and $[\theta(0), \psi(0)]' = [\frac{\pi}{12}, -\frac{\pi}{4}]'$ rad, and such that

$$\dot{x}^\star = \frac{\pi}{2}\,\mathrm{m\,s^{-1}},\ \dot{y}^\star = 0\,\mathrm{m\,s^{-1}},$$
$$\psi^\star = 0\,\mathrm{rad},\ \theta^\star = 0\,\mathrm{rad}.$$

TABLE I

QUADROTOR PARAMETERS.

m	kg	0.5
I_x	$\mathrm{kg\,m^2}$	1.5×10^{-3}
I_y	$\mathrm{kg\,m^2}$	1.5×10^{-3}
I_z	$\mathrm{kg\,m^2}$	2.8×10^{-3}
L	m	8.84×10^{-2}

Furthermore, according to [5], [22], [23], additional low frequency sinusoidal forces and moments are added as disturbance terms, which may stem e.g., from wind or surrounding magnetic sources that typically act at low frequencies.

In the considered scenario, subsystem (7a) simplifies since $d_2 = 1$, while $\delta_1 := d_x s_{x_0} - d_y c_{x_0}$, and $\delta_2 := d_x c_{x_0} + d_y s_{x_0} - x_1 u_0$. All the simulations have been executed using the automatic selection solver, fixed-time step equal to 1×10^{-3} s, which is consistent with future practical implementation of the proposal, and a simulation window of 30 s.

B. Controllers design

Making reference to subsystem (7a), the corresponding initial conditions result in $[x_0(0), x_1(0), x_2(0)]' = [-\frac{\pi}{4}, 0.5, 0.5]'$, while the control parameters are selected as $k_0 = 5$, $k_1 = 100$, $k_2 = 200$, and $\gamma = 10$. Finally, as mentioned in §III, a suitable controller has been designed for stabilizing θ to zero. More specifically, letting s be the Laplace variable, a linear controller $R_\theta(s)$ is designed as

$$R_\theta(s) = \frac{0.09 I_y (1 + 10s)}{1 + 0.1s}.$$

C. Simulation results

Figures 2 and 3 show the evolution in space of the quadrotor position $\boldsymbol{p}$, and the time evolution of the quadrotor angles θ and ψ, respectively. Moreover, in Figure 2, the evolution in time of the sliding variable s_2 and its derivative $\dot{s}_2$ is reported. The behaviour of the control inputs u_0 and u_1 is instead given in Figure 4, where one can observe that u_1 is continuous by virtue of the artificial increase of the relative degree according to (21). This is an important aspect for practical implementation in order to alleviate chattering phenomena due to the discontinuity of the control law (23). Finally, for the sake of clarity, the interval [0,0.5] s of the time evolution of x_0, x_1, and x_2, converging to zero according to the main result in §IV-D, is shown in Figure 5.

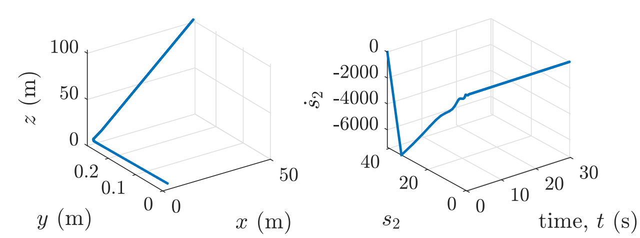

Fig. 2. Evolution in space of the quadrotor position $\boldsymbol{p}$ (left), and time evolution of the sliding variable s_2 and its derivative $\dot{s}_2$ (right).

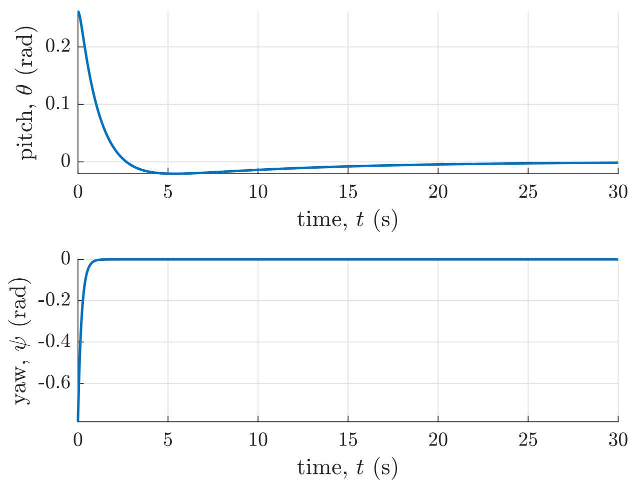

Fig. 3. Time evolution of the pitch and yaw angles θ and ψ.

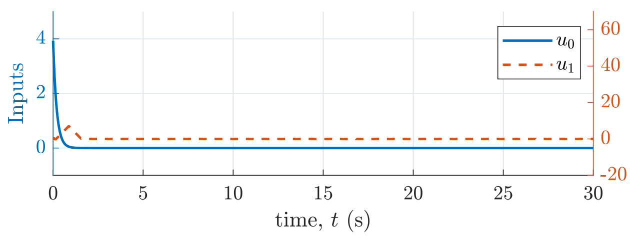

Fig. 4. Time evolution of control signals u_0 and u_1.

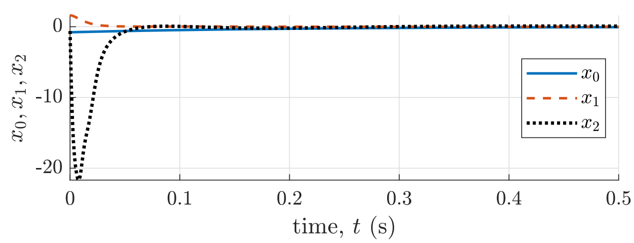

Fig. 5. Time evolution of states x_0, x_1, and x_2 in the interval [0,0.5] s.

VI. Conclusions

In this paper, a multiple-surface sliding mode control approach is proposed to solve a navigation problem for quadrotor UAVs aimed at emulating a nonholonomic-like system motion. First, the model of the quadrotor is suitably recast into a nonholonomic system framework eligible to design the proposed sliding mode control scheme. Then, a multiple-surface method is introduced and a suboptimal second order sliding mode control approach is designed and discussed. The proposal has the advantage to cope with uncertainty terms affecting the plant, for instance due to modelling mismatches and external disturbances. Finally, simulation results show the validity of the proposed strategy.

References

[1] H. Shakhatreh, A. H. Sawalmeh, A. Al-Fuqaha, Z. Dou, E. Almaita, I. Khalil, N. S. Othman, A. Khreishah, and M. Guizani, "Unmanned aerial vehicles (UAVs): A survey on civil applications and key research challenges," *IEEE Access*, vol. 7, pp. 48 572–48 634, 2019.

[2] V. Dobrokhodov, "Kinematics and dynamics of fixed-wing UAVs," in *Handbook of Unmanned Aerial Vehicles*, K. P. Valavanis and G. J. Vachtsevanos, Eds. Dordrecht: Springer Netherlands, 2015, pp. 243–277.

[3] C. Powers, D. Mellinger, and V. Kumar, "Quadrotor kinematics and dynamics," in *Handbook of Unmanned Aerial Vehicles*, K. P. Valavanis and G. J. Vachtsevanos, Eds. Dordrecht: Springer Netherlands, 2015, pp. 307–328.

[4] E. Lavretsky, "Robust and adaptive control methods for aerial vehicles," in *Handbook of Unmanned Aerial Vehicles*, K. P. Valavanis and G. J. Vachtsevanos, Eds. Dordrecht: Springer Netherlands, 2015, pp. 675–710.

[5] L. Bascetta and G. P. Incremona, "Design of sliding mode controllers for quadrotor vehicles via flatness-based feedback and feedforward linearization strategies," in *European Control Conference*, Delft, Netherlands, 2021, pp. 1622–1627.

[6] S. Formentin and M. Lovera, "Flatness-based control of a quadrotor helicopter via feedforward linearization," in *IEEE Conference on Decision and Control*, Orlando, Florida, USA, 12 2011, pp. 6171–6176.

[7] D. Falanga, P. Foehn, P. Lu, and D. Scaramuzza, "PAMPC: Perception-Aware Model Predictive Control for quadrotors," in *IEEE/RSJ International Conference on Intelligent c Robots and Systems (IROS)*, Madrid, Spain, 2018, pp. 1–8.

[8] M. Greeff and A. P. Schoellig, "Flatness-based model predictive control for quadrotor trajectory tracking," in *International Conference on Intelligent Robots and Systems*, Madrid, Spain, 2018, pp. 6740–6745.

[9] H. Castañeda and J. Gordillo, "Embedded flight control based on adaptive sliding mode strategy for a quadrotor micro air vehicle," *Electronics*, vol. 8, no. 7, pp. 1–15, 2019.

[10] P. Lu, E. van Kampen, and Q. Chu, "Nonlinear quadrotor control with online model identification," in *Advances in Aerospace Guidance, Navigation and Control*, J. Bordeneuve-Guibé, A. Drouin, and C. Roos, Eds. Cham: Springer, 2015, pp. 381–98.

[11] A. Ferrara, G. P. Incremona, and M. Cucuzzella, *Advanced and Optimization Based Sliding Mode Control: Theory and Applications*. Philadelphia, PA: Society for Industrial and Applied Mathematics, 2019.

[12] E.-H. Zheng, J.-J. Xiong, and J.-L. Luo, "Second order sliding mode control for a quadrotor UAV," *ISA Transactions*, vol. 53, no. 4, pp. 1350–1356, 2014.

[13] O. Mechali, L. Xu, Y. Huang, M. Shi, and X. Xie, "Observer-based fixed-time continuous nonsingular terminal sliding mode control of quadrotor aircraft under uncertainties and disturbances for robust trajectory tracking: Theory and experiment," *Control Engineering Practice*, vol. 111, p. 104806, 2021.

[14] O. Mofid, S. Mobayen, C. Zhang, and B. Esakki, "Desired tracking of delayed quadrotor UAV under model uncertainty and wind disturbance using adaptive super-twisting terminal sliding mode control," *ISA Transactions*, vol. 123, pp. 455–471, 2022.

[15] Y. Bouzid, B. Yasmina, H. Siguerdidjane, and M. Zareb, "Quadrotor guidance-control for flight like nonholonomic vehicles," in *International Conference on Unmanned Aircraft Systems*, Dallas, TX, USA, 2018, pp. 980–988.

[16] A.-C. Huang and Y.-C. Chen, "Adaptive multiple-surface sliding control for non-autonomous systems with mismatched uncertainties," *Automatica*, vol. 40, no. 11, pp. 1939–1945, 2004.

[17] G. Bartolini, A. Ferrara, and E. Usai, "Chattering avoidance by second-order sliding mode control," *IEEE Transactions on Automatic Control*, vol. 43, no. 2, pp. 241–246, 1998.

[18] Y. Bouzid, H. Siguerdidjane, and Y. Bestaoui, "Flight control boosters for three-dimensional trajectory tracking of quadrotor: Theory and experiment," *Journal of Systems and Control Engineering*, vol. 232, no. 6, pp. 709–727, 2018.

[19] A. Astolfi, "Discontinuous control of nonholonomic systems," *Systems & Control Letters*, vol. 27, no. 1, pp. 37–45, 1996.

[20] A. Oppenheim, A. Willsky, and S. Nawab, *Signals & Systems*. Prentice-Hall of India Private Limited, 2008.

[21] G. Bartolini, A. Ferrara, A. Levant, and E. Usai, "On second order sliding mode controllers," in *Variable Structure Systems, Sliding Mode and Nonlinear Control*, ser. Lecture Notes in Control and Information, K. D. Young and Ü. Özgüner, Eds. London: Springer-Verlag, 1999, pp. 329–350.

[22] N. Xuan-Mung and S. K. Hong, "Robust backstepping trajectory tracking control of a quadrotor with input saturation via extended state observer," *Applied Sciences*, vol. 9, no. 23, p. 5184, 2019.

[23] ——, "Robust adaptive formation control of quadcopters based on a leader-follower approach," *International Journal of Advanced Robotic Systems*, vol. 16, no. 4, 2019.